ComEX

IEICE Communications Express, Vol.10, No.10, 780–785

Generating a super-resolution radar angular spectrum using physiological component analysis

Takuya Sakamoto[1, a)]

[1] *Graduate School of Engineering, Kyoto University, Kyotodaigaku-Katsura, Nishikyo-ku, Kyoto 615–8510, Japan*

a) *sakamoto.takuya.8n@kyoto-u.ac.jp*

Abstract: In this study, we propose a method for generating an angular spectrum using array radar and physiological component analysis. We develop physiological component analysis to separate radar echoes from multiple body positions, where echoes are phase-modulated by propagating pulse waves. Assuming that the pulse wave displacements at multiple body positions are constant multiples of a time-shifted waveform, the method estimates echoes using a simplified mathematical model. We exploit the mainlobe and nulls of the directional patterns of the physiological component analysis to form an angular spectrum. We applied the proposed method to simulated data to demonstrate that it can generate a super-resolution angular spectrum.

Keywords: radar angular spectrum, pulse wave, physiological component analysis

Classification: Sensing

References

[1] S.S. Najjar, A. Scuteri, V. Shetty, J.G. Wright, D.C. Muller, J.L. Fleg, H.P. Spurgeon, L. Ferrucci, and E.G. Lakatta, "Pulse wave velocity is an independent predictor of the longitudinal increase in systolic blood pressure and of incident hypertension in the Baltimore longitudinal study of aging," *J. Am. Coll. Cardiol.*, vol. 51, no. 14, pp. 1377–1383, Nov. 2009. DOI: 10.1016/j.jacc.2007.10.065

[2] C. Holz and E.J. Wang, "Glabella: Continuously sensing blood pressure behavior using an unobtrusive wearable device," Proc. ACM on Interactive, Mobile, Wearable Ubiquitous Technol., vol. 1, no. 3, Sept. 2017. DOI: 10.1145/3132024

[3] D.B. McCombie, A.T. Reisner, and H.H. Asada, "Adaptive blood pressure estimation from wearable PPG sensors using peripheral artery pulse wave velocity measurements and multi-channel blind identification of local arterial dynamics," Proc. 2006 Int. Conf. IEEE EMBS, New York, NY, USA, pp. 3521–3524, Aug. 2006. DOI: 10.1109/IEMBS.2006.260590

[4] S.L.-O. Martin, A.M. Carek, C.-S. Kim, H. Ashouri, O.T. Inan, J.-O. Hahn, and R. Mukkamala, "Weighing scale-based pulse transit time is a superior marker of blood pressure than conventional pulse arrival time," *Sci. Rep.*, vol. 6, 39273, Dec. 2016. DOI: 10.1038/srep39273

[5] T.-H. Tao, S.-J. Hu, J.-H. Peng, and S.-C. Kuo, "An ultrawideband radar based pulse sensor for arterial stiffness measurement," Proc. 29th Ann. Int. Conf.

DOI: 10.1587/comex.2021XBL0137
Received June 29, 2021
Accepted July 7, 2021
Publicized July 14, 2021
Copyedited October 1, 2021

IEEE EMBS, Lyon, France, pp. 1679–1682, Aug. 2007. DOI: 10.1109/IEMBS.2007.4352631

[6] M.-C. Tang, C.-M. Liao, F.-K. Wang, and T.-S. Horng, "Noncontact pulse transit time measurement using a single-frequency continuous-wave radar," Proc. 2018 IEEE/MTT-S IMS, Philadelphia, PA, USA, pp. 1409–1412, June 2018. DOI: 10.1109/MWSYM.2018.8439326

[7] T. Lauteslager, M. Tømmer, T.S. Lande, and T.G. Constandinou, "Coherent UWB radar-on-chip for in-body measurement of cardiovascular dynamics," *IEEE Trans. Biomed. Circuits Syst.,* vol. 13, no. 5, pp. 814–824, Oct. 2019. DOI: 10.1109/TBCAS.2019.2922775

[8] R. Vasireddy, J. Goette, M. Jacomet, and A. Vogt, "Estimation of arterial pulse wave velocity from Doppler radar measurements: a feasibility study," 41st Ann. Int. Conf. IEEE EMBS, Berlin, Germany, pp. 5460–5464, July 2019. DOI: 10.1109/EMBC.2019.8857644

[9] L. Lu, C. Li, and D.Y.C. Lie, "Experimental demonstration of noncontact pulse wave velocity monitoring using multiple Doppler radar sensors," Proc. 2010 Ann. Int. Conf. IEEE Eng. Med. Biology, Buenos Aires, Argentina, pp. 5010–5013, Aug. 2010. DOI: 10.1109/IEMBS.2010.5627213

[10] F. Michler, K. Shi, S. Schellenberger, B. Scheiner, F. Lurz, R. Weigel, and A. Koelpin, "Pulse wave velocity detection using a 24-GHz six-port based Doppler radar," 2019 IEEE Radio and Wireless Symp., Orlando, FL, USA, Jan. 2019. DOI: 10.1109/RWS.2019.8714521

[11] Y. Oyamada, T. Koshisaka, and T. Sakamoto, "Experimental demonstration of accurate noncontact measurement of arterial pulse wave displacements using 79-GHz array radar," *IEEE Sensors J.*, vol. 21, no. 7, pp. 9128–9137, April 2021. DOI: 10.1109/JSEN.2021.3052602

[12] T. Sakamoto, "Signal separation using a mathematical model of physiological signals for the measurement of heart pulse wave propagation with array radar," *IEEE Access*, vol. 8, pp. 175921–175931, Sept. 2020. DOI: 10.1109/ACCESS.2020.3026539

1 Introduction

Pulse wave velocity (PWV) is an indicator of a variety of cardiovascular diseases [1] that is calculated by dividing the distance between two body parts by the pulse transit time (PTT), where the PTT is the time difference between the pulse arrival times measured at different body positions. In clinical practice, the body volume change caused by the pulse wave is measured to estimate the PWV. A common technique to measure the PTT is to use multiple photoplethysmogram (PPG) sensors attached to multiple parts of the subject's body [2, 3, 4].

Radar-based noncontact sensing is preferred to contact-type sensors (e.g., PPG) because it can provide unobtrusive monitoring of PWV data over long periods without causing discomfort to users. There are existing studies on radar-based pulse wave measurement [5, 6, 7, 8, 9, 10]. In [5], a radar system was placed on the patient's upper arm and left ankle. In [6], the displacements of the subject's arm and chest were measured simultaneously using a radar system. In [7], six parts of the subject's body were measured sequentially using a radar system. In all these studies [5, 6, 7], radar antennas were placed in close contact with the body.

In [8], two radar systems were placed approximately 150 mm from the subject's

DOI: 10.1587/comex.2021XBL0137
Received June 29, 2021
Accepted July 7, 2021
Publicized July 14, 2021
Copyedited October 1, 2021

chest and groin. In [9], two radar systems were placed close to the subject's chest and calf. In [10], a phased array radar system was used to measure the pulse wave at two locations in the subject's abdomen. In [11], an array radar was placed 1.2 m away from the subject, and the displacements at the back and calf were measured simultaneously. These techniques that use an array radar system require accurate signal separation so that tiny displacements at multiple body parts are estimated accurately. To improve the signal separation accuracy, [12] introduced an algorithm based on optimization with a mathematical model of physiological signals. This technique is called physiological component analysis (PHCA) and has achieved high accuracy in separating signals when the echoes are modulated by constant multiples of time-shifted displacement waveforms.

In this study, we demonstrate the applicability of PHCA to the generation of radar angular spectra that enable the estimation of the direction of arrival (DOA) of echoes. We first review the PHCA procedures concisely, and then present the proposed method to form the angular spectrum of a directional pattern. We compare the angular spectra of the PHCA and simple beamformer to demonstrate the super-resolution property of the PHCA.

2 System model

To measure physiological signals, we assume the use of a radar system with an M-element uniform linear antenna array with a spacing of $\lambda/2$, where λ is the wavelength. We model the transmitted signal as a narrow-band signal. We assume that the number of targets (body positions) is N, and that $N \leq M$ is satisfied. The line-of-sight displacement of the j-th target is $d_j(t)$ as a function of time t. The displacement vector is denoted by $\boldsymbol{d}(t) = [d_1(t), d_2(t), \cdots, d_N]^{\mathrm{T}}$. The echoes are phase-modulated by the displacement as $s_j(t) = \mathrm{e}^{\mathrm{j}2kd_j(t)}$, where $k = 2\pi/\lambda$ is the wave number. The echo vector is denoted by $\boldsymbol{s}(t) = [s_1(t), s_2(t), \cdots, s_N(t)]^{\mathrm{T}}$. Let the propagation channel matrix be A. The signal $x_i(t)$ is received at the i-th element, which forms a signal vector $\boldsymbol{x}(t) = [x_1(t), x_2(t), \cdots, x_M(t)]^{\mathrm{T}}$, where $\boldsymbol{x}(t)$ is expressed as $\boldsymbol{x}(t) = A\boldsymbol{s}(t) + \boldsymbol{n}(t)$, where $\boldsymbol{n}(t)$ is additive noise.

3 Physiological component analysis

We proposed PHCA [12] to determine an $N \times M$ matrix $W = [\boldsymbol{w}_1 \boldsymbol{w}_2 \cdots \boldsymbol{w}_N]^{\mathrm{T}}$ and estimate echoes as $\hat{\boldsymbol{s}}(t) = W\boldsymbol{x}(t)$, which leads to the estimate of the displacement $\hat{\boldsymbol{d}}(t) = (1/2k)\angle\hat{\boldsymbol{s}}(t)$, where $\angle$ denotes the argument of a complex number. Note that ambiguity is allowed in the permutation and constant multiplication when we estimate $\hat{\boldsymbol{d}}(t)$. For simplicity, we assume that N is known in advance.

In PHCA, we estimate W by solving

$$\max_{W \in \mathbb{C}^{n \times m}} F(W), \tag{1}$$

where

$$F(W) = F_1(W)F_2(W)F_3(W)F_4(W). \tag{2}$$

The objective function $F(W)$ comprises four functions that are derived from approximations based on a mathematical model of physiological signals [12]. The functions

© IEICE 2021
DOI: 10.1587/comex.2021XBL0137
Received June 29, 2021
Accepted July 7, 2021
Publicized July 14, 2021
Copyedited October 1, 2021

are defined as

$$F_1(W) = \min_{1 \le i \le N} \lambda(i)^2, \tag{3}$$

$$F_2(W) = \prod_{1 \le i < j \le N} \frac{\int_{-\infty}^{\infty} \left| g_{i,j}(\tau) \right|^4 \mathrm{d}\tau}{\left(\int_{-\infty}^{\infty} \left| g_{i,j}(\tau) \right|^2 \mathrm{d}\tau \right)^2}, \tag{4}$$

$$F_3(W) = \prod_{1 \le i < j \le N} \frac{\max_{\tau > 0} \left| g_{i,j}(\tau) \right|^2}{\max_{\tau < 0} \left| g_{i,j}(\tau) \right|^2}, \tag{5}$$

$$F_4(W) = \prod_{1 \le i < j \le N} \min\{(\boldsymbol{u}_i^{\mathrm{T}} \boldsymbol{u}_j)^{-1}, \gamma\}, \tag{6}$$

where

$$\lambda(i)^2 = \left| \int \Re[\hat{s}_i]^2 - \Im[\hat{s}_i]^2 \mathrm{d}t \right|^2 + 4 \left| \int \Re[\hat{s}_i] \Im[\hat{s}_i] \mathrm{d}t \right|^2, \tag{7}$$

$$g_{i,j}(\tau) = \int_{-\infty}^{\infty} \frac{\int_{-\infty}^{\infty} d_j(t') \mathrm{e}^{-\mathrm{j}\omega t'} \mathrm{d}t'}{\int_{-\infty}^{\infty} d_i(t') \mathrm{e}^{-\mathrm{j}\omega t'} \mathrm{d}t'} \mathrm{e}^{\mathrm{j}\omega\tau} \mathrm{d}\omega, \tag{8}$$

$$\boldsymbol{u}_i = (Q_{\mathrm{DFT}} \boldsymbol{w}_i) \circ (Q_{\mathrm{DFT}} \boldsymbol{w}_i)^*, \tag{9}$$

where we set $\gamma = 10$, Q_{DFT} is a discrete Fourier transform matrix, the symbol $\circ$ denotes the element-wise multiplication operator, and the superscript $*$ denotes the complex conjugate.

4 Proposed method to form super-resolution angular spectra

Using PHCA, we can obtain W that is optimized to extract each echo while suppressing the other interfering echoes. For simplicity, we assume $N = 2$ in this study; thus, we can form an angular spectrum $P(\theta)$ using the directional patterns $P_1(\theta)$ and $P_2(\theta)$, where $P_i(\theta)$ is a directional pattern for $\boldsymbol{w}_i$ and θ is the angle. We estimate the angular spectrum $P(\theta)$ as

$$P(\theta) = \frac{\exp(\beta(P_1(\theta) - P_0))}{P_2(\theta)} + \frac{\exp(\beta(P_2(\theta) - P_0))}{P_1(\theta)}, \tag{10}$$

where we set $\beta = 10$ and $P_0 = 0.5$ empirically.

We formulate Eq. (10) because the optimized W in PHCA forms directional patterns with the mainlobe directed to one of the DOAs and is null at the other DOAs. Thus, Eq. (10) emphasizes the central part of the mainlobe greater than -3 dB, and the null of the other directional pattern is also used.

5 Application of the proposed method

We assumed a 79 GHz array radar with $M = 6$ elements. For simplicity, we assumed $N = 2$. Body positions 1 and 2 were located at distances of x_1 and x_2 from the bottom of the antenna. We assumed that the intensities of the echoes were the same, $|s_1(t)|^2 = |s_2(t)|^2 = 1$, and that the signal-to-noise power ratio (S/N) was 45 dB. We assumed that the skin displacement waveforms $d_1(t)$ and $d_2(t)$ at body positions 1 and 2 were identical, except for a delay of 0.3 s that corresponded to the PTT, where $d_1(t)$ and $d_2(t)$ had sawtooth waves with a peak-to-peak amplitude of 100 μm, which

DOI: 10.1587/comex.2021XBL0137
Received June 29, 2021
Accepted July 7, 2021
Publicized July 14, 2021
Copyedited October 1, 2021

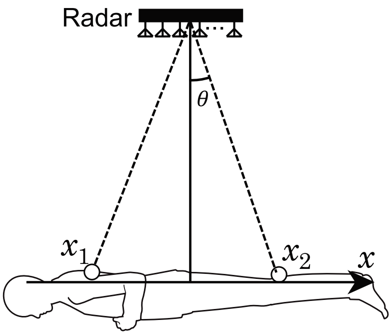

Fig. 1. System model assumed in this study.

is within a typical range for actual measurements, and the equivalent S/N for the physiological component was 21.9 dB. Figure 1 shows the assumed measurement scenario for a participant lying on a bed with an array radar placed above. We set the height of the antenna array baseline from the target human body to 1.4 m. We solved the optimization problem in Eq. (1) using a genetic algorithm with a population size of 100 and the number of generations set to 300.

Figure 2 shows the directional patterns of PHCA (upper panels) and the angular spectra (lower panels) obtained using the proposed method. We assumed two settings with $(x_1, x_2) = (-0.2\,\mathrm{m}, 0.2\,\mathrm{m})$ (scenario 1) and $(-0.1\,\mathrm{m}, 0.3\,\mathrm{m})$ (scenario 2). The actual DOAs are indicated by dashed blue lines in the figures. Note that we show P_1, P_2, and P as a function of x instead of θ for the readers' convenience. We note

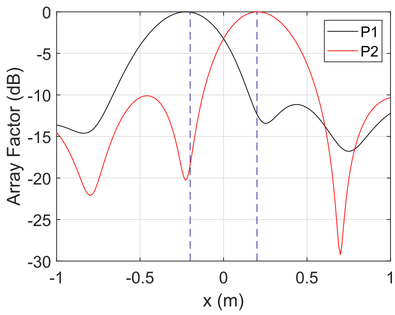

(a) Directional pattern of the PHCA in scenario 1.

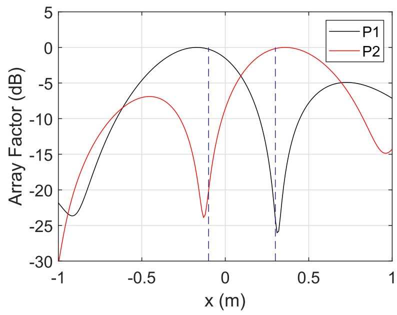

(b) Directional pattern of the PHCA in scenario 2.

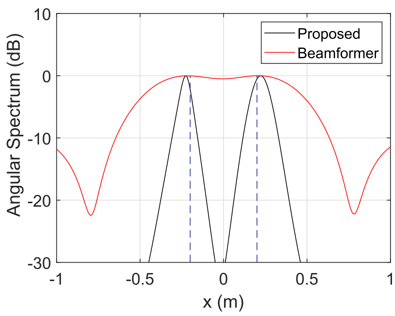

(c) Angular spectrum formed with the proposed method (scenario 1).

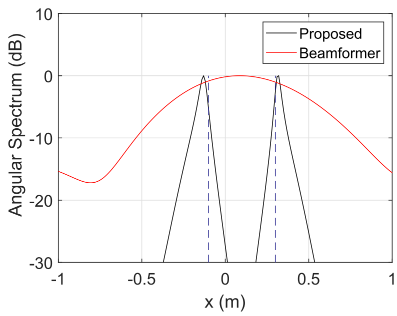

(d) Angular spectrum formed with the proposed method (scenario 2).

Fig. 2. Directional patterns and angular spectra generated using the proposed method.

DOI: 10.1587/comex.2021XBL0137
Received June 29, 2021
Accepted July 7, 2021
Publicized July 14, 2021
Copyedited October 1, 2021

that the lower panels also show the angular spectrum of the beamformer method for comparison. We observed from the figure that PHCA formed directional patterns to extract echoes while suppressing the other echo. The proposed method exploited the characteristic and generated high-resolution angular spectra. The lower panels in Fig. 2 show that the proposed method generated a super-resolution spectrum. The average error in estimating DOAs in scenario 1 and 2 were 2.5×10^{-2} m and 2.3×10^{-2} m. The errors in estimating the distance between the two body positions were 4.6×10^{-2} m and 4.7×10^{-2} m in scenarios 1 and 2, respectively, which resulted in a relative error of 12% in both scenarios.

Although we assumed that the number of targets was known, it is important to investigate the performance of the proposed method when the number of targets is unknown. It is also important to study the accuracy and resolution limit of the proposed method under various conditions, including various DOAs, S/Ns, displacement waveforms, and numbers of elements. Furthermore, it is important to compare the proposed method with existing super-resolution methods of adaptive array processing. We will consider these additional issues in our future work.

6 Conclusion

In this study, we proposed a method for generating a radar angular spectrum using PHCA directional patterns. PHCA is an approach to automatically separate signals based on a mathematical model of pulse wave propagation. The formation of the angular spectrum allows us to locate the body positions that exhibit pulse wave displacement, which results in the estimation of the distance between body positions. The simulation results showed an average error of 12% for estimating the distance between two body positions. Because the calculation of PWV requires the distance of the propagation path, we expect DOA estimation using the proposed method to be applied in healthcare and medical applications.

Acknowledgments

This work was supported in part by JSPS 19H02155, JST JPMJPR1873, and JST COI JPMJCE1307.

DOI: 10.1587/comex.2021XBL0137
Received June 29, 2021
Accepted July 7, 2021
Publicized July 14, 2021
Copyedited October 1, 2021